JOURNAL OF MATERIALS SCIENCE 26 (1991) 5521–5526

Tetragonal-to-monoclinic phase transformation during thermal cycling and isothermal ageing in yttria–partially stabilized zirconia

H. TSUBAKINO, M. HAMAMOTO, R. NOZATO
Himeji Institute of Technology, Shosha, Himeji 671-22, Japan

The tetragonal-to-monoclinic (T → M) phase transformation accompanied with thermal cycling has been studied by ionic conductivity, dilatation and X-ray diffraction measurements. With repeating thermal cycling, the M_s point shifts to a higher temperature, the amount of expansion due to T → M transformation increases, and the transformation proceeds from the surface in the specimen interiors. These phenomena are attributed to grain boundary cracking which occurs as a result of the transformation. The time-transformation isotherms at 353 K and at room temperature can be expressed by the Johnson–Mehl equation $f = 1 - \exp(-bt^n)$, and the same n value of 0.7 was obtained irrespective of grain size and of environment.

1. Introduction

Partially stabilized zirconia ceramics have remarkable advantages in mechanical properties, such as bending strength and fracture toughness. This improvement in mechanical properties is believed to be related to the martensitic transformation from tetragonal to monoclinic structures, i.e. a transformation-toughened mechanism [1].

However, these ceramics show an unusual degradation phenomenon during ageing relatively low temperatures (423–673 K), as reported by Kobayashi *et al.* [2]. Many investigators have studied this degradation phenomenon and agree that degradation is due to the occurrence of cracking as a result of partial transformation from tetragonal (T) to monoclinic (M) structure during ageing [2–13]. These T–M transformation phenomena are complicated and are affected by many factors. Firstly, the transformation depends strongly on grain size [4–6], i.e. the transformation does not take place in ceramics less than a critical grain size of about 0.3 [4] or 0.5 μm [5]. Secondly, the transformation is enhanced when the ceramics are exposed to the environment of water vapour [6–12]. Thirdly, the transformation is enhanced by cyclic annealing [7, 13]. In addition, the content of solute (Y_2O_3) and the addition of other oxides such as CeO_2 and Al_2O_3 also affect the transformation rate [3, 11, 14, 15].

In this study, the propagation phenomena and kinetics of T–M transformation in ZrO_2–3 mol % Y_2O_3 during thermal cycling and during isothermal ageing at relatively low temperatures (below 373 K) are investigated, in order to gain information on the T–M transformation and to prevent the degradation phenomenon.

2. Experimental procedure

The zirconia powder containing 3 mol % yttria was prepared by a co-precipitation method. The chemical composition of the powder is shown in Table I. The powder was uniaxially pressed at 100 MPa and the compacts were sintered in open air for 18 ks at temperatures ranging from 1573 to 1973 K (T_s), followed by cooling down to 1100 K at 1.3 K s^{-1}, and then air-cooled to avoid cracks caused by the martensitic transformation [7]. The sintered specimens were discs 9.4 mm in diameter and about 2 mm thick, and rectangular bars of 3 × 2.7 × 9 mm.

Ionic conductivity was measured by means of a two-probe d.c. method during cooling, at a rate of 0.022 K s^{-1} from 1073 to about 373 K. Platinum paste was coated on both sides of the discs, followed by heating to 1273 K. Spring-loaded platinum wires ensured good electrical contact with the specimen. The current at the applied potential of 1 ± 0.0015 V was recorded as a function of temperature. These conductivity measurements were performed in open air. Thermal expansion was measured during the heating–cooling (thermal) cycle in the temperature range from room temperature to 1073 K, at the same rate as in the conductivity measurements. The specimen holders of the dilatometer were of quartz. The expansion of the quartz tube was neglected in these measurements because the expansion coefficient of quartz is about 1/30 that of the specimens.

0022–2461/91 $03.00 + .12

TABLE I Chemical composition of ZrO_2–3 mol % Y_2O_3 powder (mass %)

Y_2O_3	CaO	MgO	SiO_2	Fe_2O_3	Al_2O_3	TiO_2
5.63	0.09	0.10	0.10	0.01	0.02	0.15

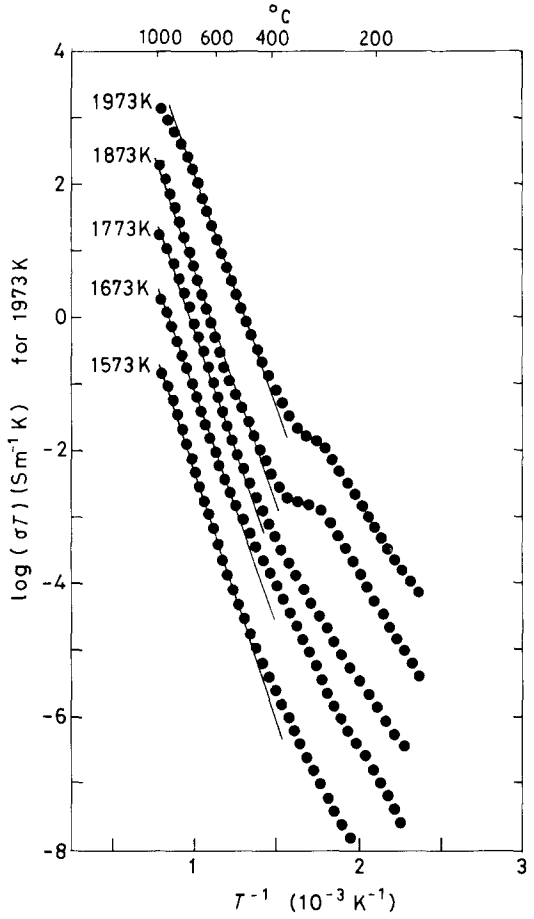

Figure 1 Electric conductivity curves during the cooling stage in ZrO_2–3 mol % Y_2O_3 sintered at various temperatures. The data are moved down one order along the longitudinal axis, accompanying a decrease in sintering temperature. Cooling rate = 0.022 K s^{-1}.

Scanning electron microscope (SEM) and the X-ray diffraction (XRD) observations were also performed. From XRD, the percentage of the monoclinic phase in the specimens was estimated from the relative intensities of the two monoclinic peaks $(1\ 1\ 1)_m + (1\ 1\ \bar{1})_m$ and the tetragonal peak $(1\ 1\ 1)_t$ + cubic peak $(1\ 1\ 1)_c + (1\ 1\ 1)_m + (1\ 1\ \bar{1})_m$.

3. Results and discussion

3.1. Tetragonal-monoclinic transformation during thermal cycling

The changes in ionic conductivity during cooling are shown in Fig. 1. The conductivity data can be given by the following equation [16] for a particular temperature range:

$$\sigma T = A \exp(-Q/RT) \quad (1)$$

where σ is the conductivity, T the temperature, A a constant, Q the activation energy and R the gas constant. The conductivity plots of the specimens sintered at 1973 and 1873 K indicate clear increases at

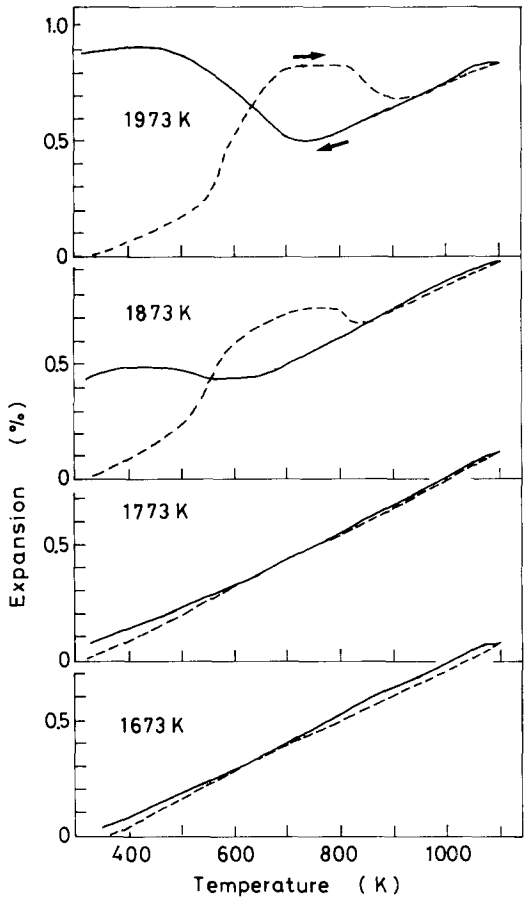

Figure 2 Dilatation curves during heating (----) and cooling (———) stages in ZrO_2–3 mol % Y_2O_3 sintered at various temperatures..

a temperature range from 700 to 600 K. However the plots of specimens sintered below 1773 K show only a small deviation to higher values from the extrapolation of data at higher temperatures. These increases and deviations are due to the T → M transformation, as suggested in a previous study [17]. Fig. 2 shows dilatation against temperature curves during thermal cycling. These curves are similar to the results for ZrO_2–2.5 mol % Y_2O_3 published by Yoshikawa *et al.* [13]. The dilatation curves of specimens sintered at 1973 and 1873 K show a distinct expansion due to the T → M transformation [13] at 700–500 K during the cooling stage, but those sintered below 1773 K show no such expansion. These results are in fairly good agreement with those in Fig. 1. It is shown in Fig. 3 that the T–M transformation can occur in specimens with larger grain sizes than about 0.3 μm (the critical grain size), which agrees well with previous studies [4–6].

Fig. 4 shows the effect of the number of thermal cycles on the behaviour of T–M transformation. The total expansion due to the T → M transformation increases with cycle number. In addition, the M_s point (the starting temperature of T → M transformation) shifts to a higher temperature, from 600 to 710 K, as cycle number increases in both specimens sintered at 1873 and 1973 K. However, the A_s point (the starting temperature of M → T transformation) is kept at almost the same temperature of about 790 K, irrespective of cycle number. These M_s and A_s points are

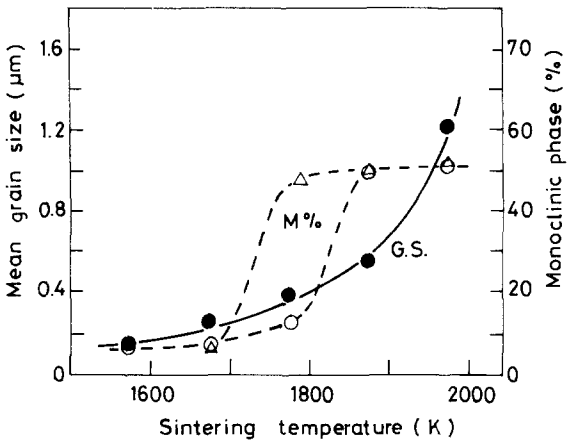

Figure 3 Mean grain size and amount of monoclinic phase for ZrO_2–3 mol % Y_2O_3 after ○, first and △, second thermal cycles against sintering temperature.

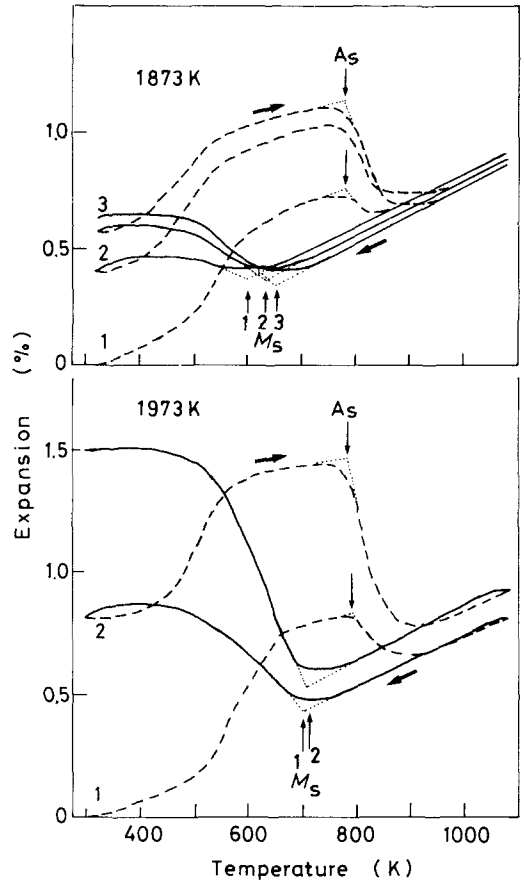

Figure 4 Dilatation curves for ZrO_2–3 mol % Y_2O_3 during thermal cycling experiments. Numbers times of thermal cycling. M_s = starting temperature of T → M transformation; A_s = starting temperature of M → T transformation.

determined from the cross-points of two extrapolated lines of the linear portions of the curves, as shown in Fig. 4. The behaviour of M_s as a function of thermal cycle number is also confirmed from ionic conductivity measurements, as shown in Fig. 5.

SEM observations of the specimen surface after the second thermal cycle indicate that cracks have occurred at grain boundaries, as shown in Fig. 6. This specimen surface was polished and etched thermally for 300 s at 1773 K prior to the thermal cycling experiments.

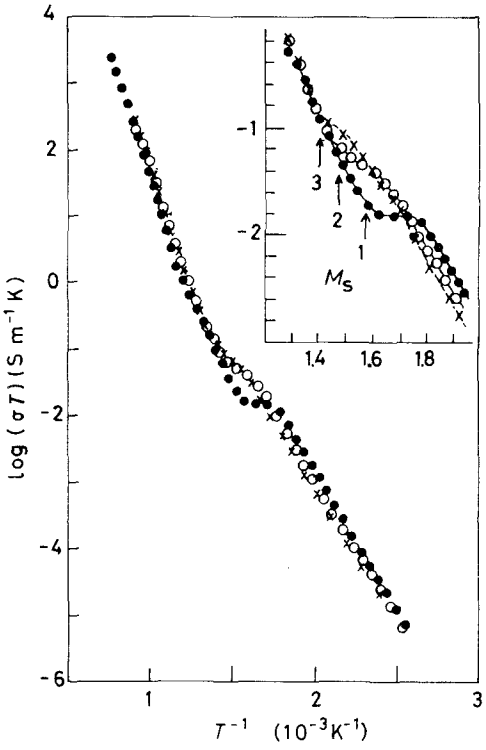

Figure 5 Conductivity curves during the cooling stage at various thermal cycles: ●, first; ○, second; ×, third. T_s = 1873 K; cooling rate = 0.022 K s^{-1}.

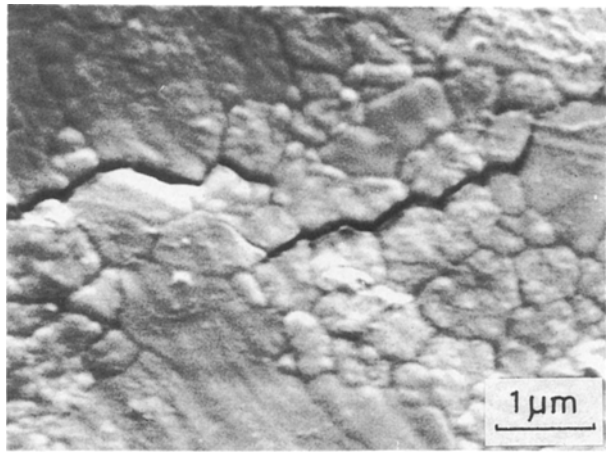

Figure 6 SEM micrograph showing grain-boundary cracks occurring at the specimen surface after the second cycle (T_s = 1873 K).

Fig. 7 shows that the T → M transformation propagates from the surface into the interior of specimen with increasing cycle number. Presumably this propagation will accompany the grain-boundary cracking, i.e., transformation-induced cracking.

The thermodynamic temperature for the transformation, T_o, is defined as the temperature at which $\Delta G_c^{T-M} = 0$, i.e. two chemical free energies of the tetragonal and monoclinic phases are equal ($G_c^T = G_c^M$), and T_o is taken as $(M_s + A_s)/2$ [18]. The martensitic transformation cannot usually start at T_o, but starts at a lower temperature than T_o, i.e. supercooling ($T_o - M_s$) is necessary for the onset of the transformation. This supercooling problem in ZrO_2 is treated by Lange [19] as follows:

$$\Delta G_{T-M} = -\Delta G_c + \Delta G_{se} + \Delta G_s = 0 \qquad (2)$$

where ΔG_c is the change in chemical free energy between the T and M phases, ΔG_{se} is the change in strain energy associated with the transformed M phase and surrounding T phase, and ΔG_s is the change in surface energy associated with the T → M transformation. Both the terms ΔG_s and ΔG_{se}will be related to the constrained term of the surrounding matrix resulting from the expansion of martensite formation.

However, TEM observations of T–M transformation [20, 21] indicate that this transformation is a nucleating controlled reaction, and the martensite laths nucleate at grain boundaries and propagate through grains. In addition, the microcracks and/or cracks are observed at grain boundaries, and are presumably due to the T → M transformation [10, 22, 23].

The cracks and/or microcracks produce free surfaces in the interior of specimens and act for the formation of strain-less martensite during the following cooling stage, and thus the term of ΔG_{se} becomes small. Furthermore, the free surface of the matrix will easily cause further nucleation of martensite laths at much deeper positions from the surface of specimens, because the constrained term of the surrounding matrix becomes less. The results obtained in this study, i.e. that the M_s shifts to higher temperature; the amount of expansion due to T → M transformation increases; and the transformation proceeds from the surface in the interiors of specimens accompanying the cyclic number, can be interpreted as the effects of grain-boundary cracking as discussed above. Therefore it can be concluded that the increase in the cohesion of grain boundaries will be the most important factor in preventing the propagation of the T → M transformation from the surface in the interiors of specimens. Then we can propose that the following term including the cohesive energy of grain boundary, ΔG_{gb}, should be added to ΔG_{T-M}:

$$\Delta G_{T-M} = -\Delta G_c + \Delta G_{se} + \Delta G_s + \Delta G_{gb} \quad (3)$$

The highest M_s point and A_s point obtained in this study are plotted in Fig. 8. In this figure, the T_0 temperatures obtained from dilatometric measurements with the arc-melted specimens [24] are also plotted. The T_0 temperature obtained from $(M_s + A_s)/2$ is about 730 K in this study. This temperature is equivalent to the Y_2O_3 content of about 1.6 mol % from the extrapolated line of the published T_0. This content is close to that at the T/(T + C) phase boundary at around 1900 K noted by Scott [25], but is smaller than that found by Ruh *et al.* [26]. The M_s point may increase further for the formation of stress-free martensite.

3.2. Isothermal kinetics of T–M transformation

Fig. 9 shows the relationship between the amount of monoclinic phase formed at the specimen surface and the ageing time in distilled water at 353 K. The enhancement of the transformation by water vapour above 423 K has been widely studied, and several

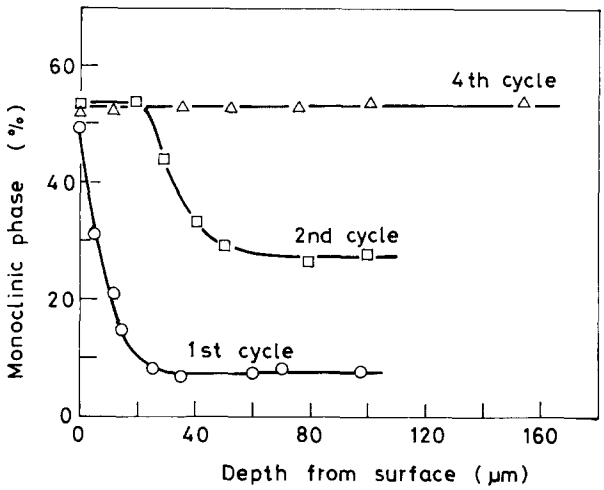

Figure 7 Relation between amount of monoclinic phase and depth from surface for ZrO_2–3 mol % Y_2O_3 after various thermal cycles. T_s = 1873 K.

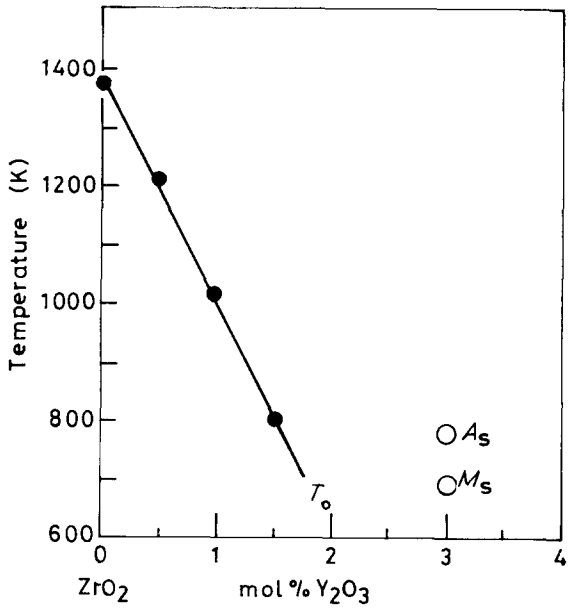

Figure 8 T ⇌ M transformation temperature of ZrO_2 as a function of Y_2O_3 concentration. ●, [24]; ○, present work.

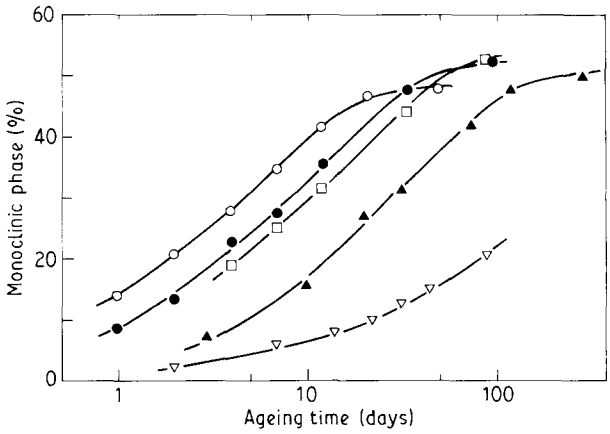

Figure 9 Relation between the amount of monoclinic phase transformed at the specimen surface and ageing time in water at 353 K. T_s = ○, 1973; ●, 1873; □, 1773; ▲, 1673; ▽, 1573 K.

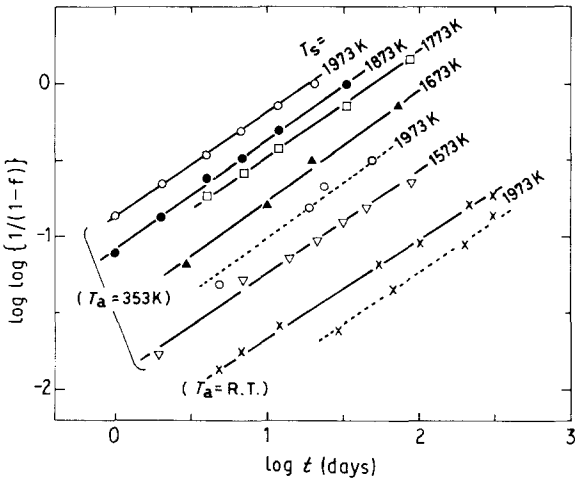

Figure 10 Plots of $\log[1/(1-f)]$ against $\log t$. Specimens aged in (– – –) air; (———) water. $n = 0.7$.

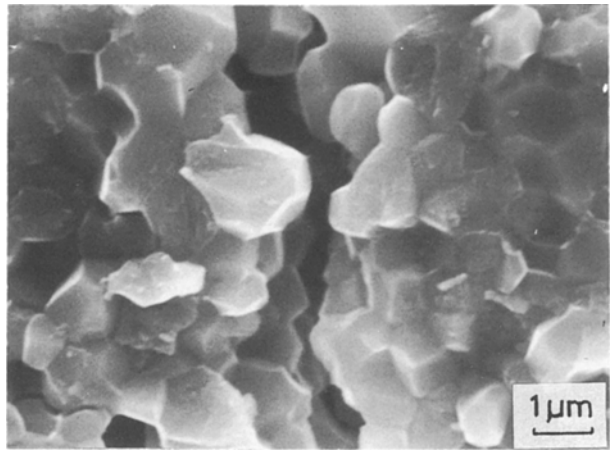

Figure 11 SEM micrograph showing grain-boundary cracks in a specimen aged in water at 353 K for 20 days (T_s = 1873 K).

enhancement models have been proposed [6–9]. The plots of specimens at each sintering temperature show typical sigmoidal curves. These results indicate that the T–M transformation proceeds isothermally, as suggested by Nakanishi *et al.* [7]. The tendency of this isothermal transformation phenomenon can be inferred from the results achieved during the heating stage of Figs 2 and 4, i.e., the expansion phenomena around 500–600 K.

The many time-transformation isotherms in alloy systems have been described by the Johnson–Mehl equation [27]:

$$f = 1 - \exp(-bt^n) \quad (4)$$

where f is the fraction of transformation, t is time, and b and n are constants. Equation 4 can be written in the following form:

$$\log\log[1/(1-f)] = n\log t + \log(b/2.3) \quad (5)$$

The plots of $\log\log[1/(1-f)]$ against ageing time are shown in Fig. 10. In this study, f was obtained from the fraction in the saturated amount of the monoclinic phase (about 52 %) shown in Figs 7 and 9. An approximately linear relationship between them is found. This fact may indicate that a certain diffusional reaction has taken place in the T → M transformation. From the slope of the straight lines, about 0.7 is obtained as the n value, irrespective of grain size and of the environments of air (dotted line) and water (solid line). From the latter results, it can be concluded that the transformation mechanism in the specimens exposed to air will be same as that in the specimens aged in water. The humidity in the air should act for the isothermal transformation. There is at present no information on the n value for the martensitic transformation, although detailed analysis on the n value may be necessary to study the nucleation stage of the transformation for the prevention of degradation.

Fig. 11 shows the grain-boundary cracking which occurred in the specimen during ageing in water for 20 days at 353 K. The energy concerning the cohesion of grain boundaries will also be important for the T–M transformation during isothermal ageing.

It can be seen in Fig. 9, in addition, that the specimen sintered at 1573 K transforms at prolonged ageing in water at 353 K, i.e. the transformation can occur even in a specimen with a mean grain size of 0.18 μm.

4. Conclusions

1. The T–M transformation is affected by several factors, such as grain size, thermal history and environment of water, but the transformation proceeds in specimens of grain size even below 0.2 μm when aged in water at 353 K.

2. As thermal cycle number increases, the M_s point (the starting temperature of the T → M transformation) shifts to a higher temperature, the amount of expansion due to the T → M transformation increases, and the transformation proceeds from the surface to the interior of specimens. These phenomena are attributed to the appearance of grain-boundary cracking.

3. The relation between the amount of T → M transformation at the specimen surface, and the time aged at 353 K and at room temperature, can be expressed by the Johnson–Mehl equation: $f = 1 - \exp(-bt^n)$, and the value of n obtained was 0.7, irrespective of grain size or of environment.

4. The grain-boundary cohesion of ZrO_2–3 mol % Y_2O_3 is the important factor for the prevention of propagation of T → M transformation into the interiors of specimens.

References

1. N. CLAUSSEN and M. R. RÜHL, in "Science and Technology of Zirconia", edited by A. H. Heuer and W. Hobbs (American Ceramics Society, Columbus, Ohio, 1981) p. 137.
2. K. KOBAYASHI, H. KUWAJIMA and T. MASAKI, *Solid State Ionics* **3/4** (1981) 489.
3. T. SATO and M. SHIMADA, *J. Amer. Ceram. Soc.* **67** (1984) C-212.
4. T. K. GUPTA, F. F. LANGE and J. H. BECHTOLD, *J. Mater. Sci.* **13** (1978) 1464.
5. H-Y. LU and S-Y. CHEN, *J. Amer. Ceram. Soc.* **70** (1987) 537.
6. T. SATO, S. OHTANI and M. SHIMADA, *J. Mater. Sci.* **20** (1985) 1466.

7. N. NAKANISHI, T. SHIGEMATSU, T. SUGIMURA and H. OKINAKA, *Zirconia Ceram.* **8** (1986) 71.
8. F. F. LANGE, G. L. DUNLOP and B. I. DAVIS, *J. Amer. Ceram. Soc.* **69** (1986) 237.
9. M. YOSHIMURA, T. NOMA, K. KAWABATA and S. SOMIYA, *J. Mater. Sci. Lett.* **6** (1987) 465.
10. K. NAKAJIMA, K. KOBAYASHI and Y. MURATA, in "Science and Technology of Zirconia II", edited by N. Claussen, M. Rühle and A. H. Heuer (American Ceramics Society, Columbus, Ohio, 1984) p. 399.
11. T. SATO and M. SHIMADA, *J. Mater. Sci.* **20** (1985) 3988.
12. S. SATO, S. OHTANI, T. ENDO and M. SHIMADA, *J. Amer. Ceram. Soc.* **68** (1985) C-320.
13. N. YOSHIKAWA and H. SUTO, *Trans. JIM* **26** (1985) 280.
14. H. WATANABE and M. CHIGASAKI, *Yogyo-Kyokaishi* **94** (1986) 255.
15. M. KIHARA, T. OGATA, K. NAKAMURA and K. KOBAYASHI, *J. Jpn Ceram. Soc.* **96** (1988) 646.
16. W. D. KINGERY, H. K. BOWEN and D. R. UHLMANN, in "Introduction to Ceramics", 2nd edn (Wiley, New York, 1976) p. 847.
17. H. TSUBAKINO, M. HAMAMOTO and R. NOZATO, *J. Mater. Sci. Lett.* **8** (1989) 295.
18. L. KAUFMAN and M. COHEN, in "Progress in Metal Physics", Vol. 7, edited by B. Chalmers and R. King (Pergamon, London, 1958) p. 165.
19. F. F. LANGE, *J. Mater. Sci.* **17** (1982) 225.
20. R-R. LEE and A. H. HEUER, *J. Amer. Ceram. Soc.* **71** (1988) 694, 701.
21. M. RÜHLE and A. H. HEUER, in "Advances in Ceramics, II" (American Ceramics Society, Columbus, Ohio, 1984) p. 14.
22. M. RÜHLE, N. CLAUSSEN and A. H. HEUER, *ibid.* p. 352.
23. T. SATO and M. SHIMADA, *J. Amer. Ceram. Soc.* **68** (1985) 356.
24. N. YOSHIKAWA and H. SUTO, *J. Jpn Inst. Metals.* **50** (1986) 108.
25. H. G. SCOTT, *J. Mater. Sci.* **10** (1975) 1523.
26. R. RUH, K. S. MAZAIYASNI, P. G. VALANTINE and H. O. BIELSTEIN, *J. Amer Ceram. Soc.* **67** (1984) C-190.
27. J. W. CHRISTIAN, in "The Theory of Transformations in Metals Alloys" (Pergamon, Oxford, 1965) p. 471.

Received 19 April 1990
and accepted 15 January 1991